

Influence of random roughness on cantilever resonance frequency

O. Ergincan and G. Palasantzas*

Zernike Institute for Advanced Materials, University of Groningen, Nijenborgh 4, 9747 AG Groningen, The Netherlands

(Received 19 August 2010; published 19 October 2010)

In this paper we investigate the influence of random roughness on the oscillation frequency of cantilevers coated with thin film overlayers. First the theory expressions for the roughness-induced frequency shift are derived using the cantilever equation of motion. Subsequently it is shown that the roughness induced shift depends on the particular roughness parameters, assuming the general case of self-affine rough surfaces for the overlayer film, the material properties of the overlayer film, and the dimensions mainly of the bare cantilever. Indeed it is shown that the roughness influence becomes significant for relatively thin cantilevers ($\leq 1 \mu\text{m}$), and increased local surface slopes (> 0.5) within the limits of applicability of the proposed formalism. The results of this study can be used in high precision frequency sensing applications in the field of micro/nanomechanics.

DOI: [10.1103/PhysRevB.82.155438](https://doi.org/10.1103/PhysRevB.82.155438)

PACS number(s): 68.35.Ct, 68.35.Gy, 68.65.Hb, 82.45.Fk

I. INTRODUCTION

Currently there is intense research with micro/nanoelectromechanical systems (MEMS/NEMS) since they are important electromechanical devices compatible with high speed and large-scale integration of silicon-based microelectronics systems. Therefore, many research groups are investigating various aspects of MEMS/NEMS in order to understand their resonance properties and potential for a wide variety of sensing applications.^{1,2} Indeed, microcantilevers, which have been used as physical, chemical, and biological sensors,³ have high sensitivity allowing mass resolution down to femtograms even in air environment.³ The sensitivity is determined by the effective vibratory mass of the resonator (depending on geometry, configuration, and material properties of the resonant structure) and the stability of the device resonance frequency.¹

As the size of cantilevers is scaled down in dimensions the surface to volume ratio increases making the influence of surfaces, and as a result that of surface roughness, important for the associated surface stress,⁴⁻⁶ and in more general the cantilever sensitivity. On the other hand during the determination of the cantilever vibration frequency and deflection only flat planar surfaces are assumed while real cantilever surfaces can be rough over various length scales. In this respect it has been shown that the adsorption-induced surface stress depends on the cantilever surface roughness.^{7,8} Cantilever deflection enhancement was found due to molecular adsorption onto cantilevers with rough surfaces.⁷ Differences in hydrogen absorption rates were associated with the dependence of surface stress on surface roughness.⁸ Nanoscale roughness was also associated with decrement of the adsorption-induced surface stress as compared to smooth surfaces.⁹

Besides cantilever sensing based on static deflection detection, cantilever sensors also operate in a dynamic mode by measuring the change in the resonance frequency. Recently it was shown that surface roughness can shift the resonance frequency of microcantilevers, depending on the properties of the surface stress, the local surface inclination using only deterministic sinusoidal rough profiles, and the Poisson ratio (ν) of the bare cantilever material.¹⁰

However, calculations of the roughness effects on the cantilever sensitivity as a function of characteristic parameters of random rough surfaces, which is a more realistic morphology for deposited metal overlayers, are still missing. Moreover, the former calculations ignored the effects of the overlayer thickness (d) and Young modulus (E).¹⁰ These are essential omissions and they will be the topic of the present paper, where, however, a more rigorous formalism will be developed, and proper random roughness models will be implemented for quantitative results.

II. THEORY FOR FREQUENCY SHIFT CALCULATION FOR CANTILEVERS WITH ROUGH SURFACES

A. Equation of cantilever motion

Here we will present briefly the theory of cantilever¹⁰ bending including the general roughness corrections form and afterward we will implement the specifics of random self-affine roughness. As in Ref. 10 we consider a thin layer of thickness d having a rough profile $h(r)$, which is deposited on top of a cantilever of thickness $d_{ca} \gg d$ [Fig. 1(a)]. Typical material for a bare cantilevers as in Fig. 1(a) is Si and in many cases the overlayer film is gold with granular roughness as shown in Fig. 1(b). The Young modulus, density, and Poisson ratio of the substrate are E_s , ρ_s , and ν_s , respectively, and these of the overlayer film are E_f , ρ_f , and ν_f . The rough surface of the deposited overlayer film is under surface stress τ , which for isotropic surfaces can be written as $\tau = \tau_o + \tau_s$. τ_o is the constant residual surface stress, and $\tau_s = 2\mu_s \epsilon_s + \lambda_s (\text{tr} \epsilon_s) I$ is the strain-dependent surface stress.^{10,11} I is the unit tensor in a two-dimensional space, and μ_s and λ_s are the isotropic Lamé surface moduli, and $\text{tr}(\epsilon_s)$ is denoting the trace of the stress tensor ϵ_s .

Based on the Bernoulli-Euler assumption with $d \ll d_{ca}$ (considering the midplane at $z = -d_{ca}/2$), the displacement field in the x direction can be written as $u(x) = u_o(x) - (z + d_{ca}/2) \partial_x Z$ (Ref. 10) (the displacement in the y direction is neglected). $Z = Z(x)$ is the displacement in the z direction. Since the bending caused by the change in the surface stress

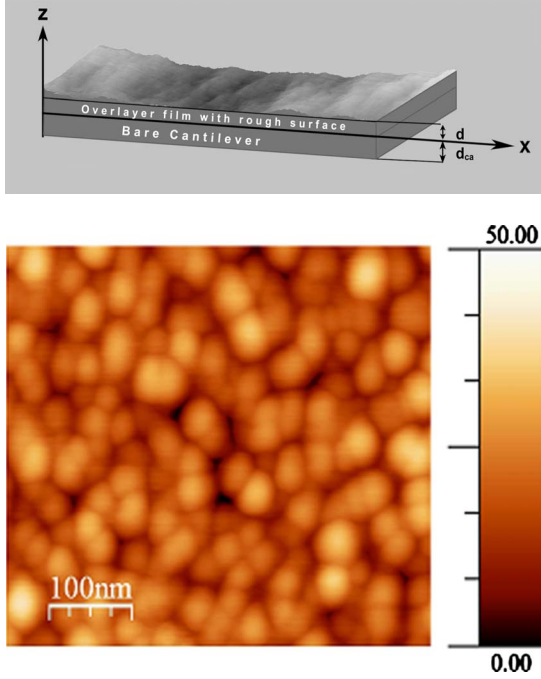


FIG. 1. (Color online) (a) Cantilever schematic with an overlayer film on top (adapted from a Si surface) and (b) granular film of Au typically deposited onto cantilevers with roughness ratio $w/\xi=0.23$ and $H=0.9$

is dominant, the overall stretching of the cantilever is neglected or equivalently $u_o(x)=0$.¹⁰ The strain components are given by $\epsilon_{xx}=\partial_x u(x)=-\left(z+d_{ca}/2\right)\partial_{xx}^2 Z$ and $\epsilon_{yy}=0$, while the Hook's law yields the corresponding stress components $\sigma_{xx}=\tilde{E}\epsilon_{xx}$ with $\tilde{E}=E/(1-\nu^2)$.¹⁰ The surface strain ϵ_s can be calculated by a coordinate transformation from the global coordinate system to the local inclined one at $z=h(r)$.¹⁰ Implementing this into the kinetic and elastic energies and further assuming the Hamilton's variational principle, as well as $n(=d/d_{ca})\ll 1$ the equation of cantilever motion has been shown to have the form [see also in Appendix Eq. (A1)] (Ref. 10).

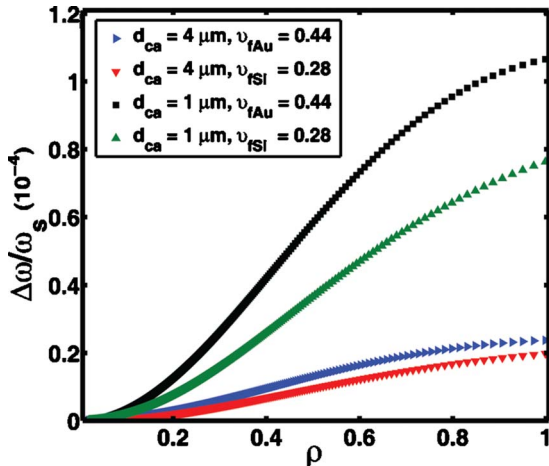


FIG. 2. (Color online) $\Delta\omega/\omega_s$ vs local surface slope for an overlayer film thickness $d=100$ nm and cantilever thicknesses (d_{ca}) 1 and 4 μm for gold ($\nu_{fAu}=0.44$) and Si ($\nu_{fSi}=0.28$).

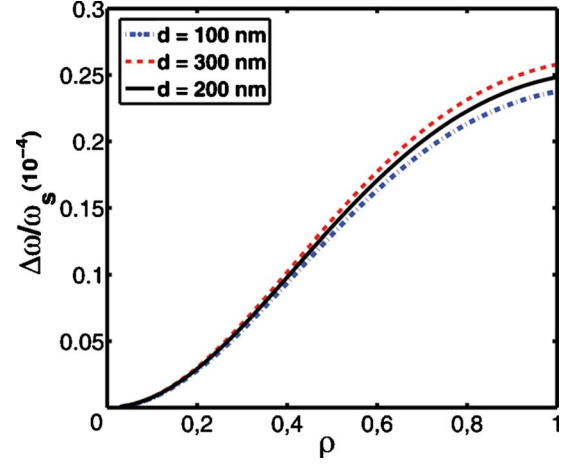


FIG. 3. (Color online) $\Delta\omega/\omega_s$ vs local surface slope for various overlayer film thickness of gold (d) and fixed cantilever thickness $d_{ca}=1$ μm .

$$\begin{aligned} & \left[\frac{\tilde{E}_s d_{ca}^3}{12} + \frac{\tilde{E}_f d_{ca}^3}{3} \left[\left(n + \frac{1}{2} \right)^3 - \frac{1}{8} \right] \right. \\ & \left. + (2\mu_s + \lambda_s) d_{ca}^2 \left(n + \frac{1}{2} \right)^2 \frac{\{1 - [v_f/(1-v_f)]\rho^2\}^2}{[1 + \rho^2]^{3/2}} \right] \frac{\partial^4 Z}{\partial x^4} \\ & + d_{ca}(\rho_s + \rho_f n) \frac{\partial^2 Z}{\partial t^2} = 0 \end{aligned} \quad (1)$$

with $\rho = \sqrt{\langle (\nabla h)^2 \rangle}$ the so called average local surface slope. Note that the assumption of a slow variation in the surface slope means relatively weak surface roughness or $\rho < 1$.

B. Frequency shift calculation

Furthermore, in order to obtain the frequency shift due to roughness, Eq. (1) can be written in the form

$$\frac{\tilde{E}_{sf,r} d_{ca}^3}{12} \frac{\partial^4 Z}{\partial x^4} + \tilde{\mu} \frac{\partial^2 Z}{\partial t^2} = 0 \quad (2)$$

with

$$\begin{aligned} \tilde{E}_{sf,r} = & \left[\tilde{E}_s + 4\tilde{E}_f \left[\left(n + \frac{1}{2} \right)^3 - \frac{1}{8} \right] + (2\mu_s + \lambda_s) \right. \\ & \left. \times \frac{12}{d_{ca}} \left(n + \frac{1}{2} \right)^2 \frac{\{1 - [v_f/(1-v_f)]\rho^2\}^2}{[1 + \rho^2]^{3/2}} \right] \end{aligned} \quad (3)$$

and $\tilde{\mu} = d_{ca}(\rho_s + \rho_f n)$. For the case of flat surfaces or equivalently $\rho=0$, Eq. (2) yields

$$\frac{\tilde{E}_{sf,s} d_{ca}^3}{12} \frac{\partial^4 Z}{\partial x^4} + \tilde{\mu} \frac{\partial^2 Z}{\partial t^2} = 0 \quad (4)$$

with $\tilde{E}_{sf,s} = [\tilde{E}_s + 4\tilde{E}_f \{ (n+1/2)^3 - 1/8 \} + (2\mu_s + \lambda_s)(12/d_{ca})(n+1/2)^2]$.

The vibration frequency of the cantilever beam is given by $\omega_r^2 = C \tilde{E}_{sf,r} (d_{ca}^3/12) / \tilde{\mu}$ with C a constant depending on geometry.¹² For flat surfaces a similar equation applies yield-

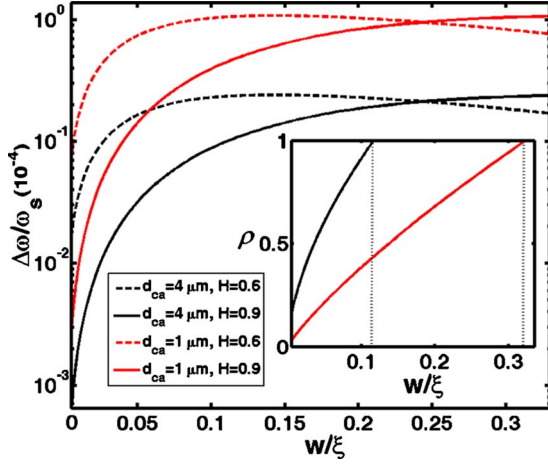


FIG. 4. (Color online) $\Delta\omega/\omega_s$ vs roughness ratio w/ξ for different roughness exponents H , overlayer thickness of a gold film $d = 100$ nm thick, and cantilever thickness $d_{ca} = 1 \mu\text{m}$. The inset shows the local surface slope ρ as a function of w/ξ for the same roughness exponents $H=0.6$ (black line) and $H=0.9$ (red line/light colored-line).

ing $\omega^2 = C\tilde{E}_{sf,s}(d_{ca}^3/12)/\tilde{\mu}$. If the roughness contributes a frequency shift $\Delta\omega$ so that $\omega_r = \omega + \Delta\omega$, then we obtain $\omega_r^2 \approx \omega^2 + 2\omega\Delta\omega$ (assuming $\Delta\omega \ll \omega$). Substitution yields the frequency shift $\Delta\omega/\omega$ with respect to that of a film/cantilever with flat surface (see also second part of the Appendix)

$$\frac{\Delta\omega}{\omega} = \frac{\tilde{E}_{sf,r} - \tilde{E}_{sf,s}}{2\tilde{E}_{sf,s}}. \quad (5)$$

Substitution of the terms $\tilde{E}_{sf,r(s)}$ yields the analytic form for the frequency shift

$$\frac{\Delta\omega}{\omega} = \left[\frac{2\mu_s + \lambda_s}{\tilde{E}_{sf,s}} \frac{6}{d_{ca}} \left(n + \frac{1}{2} \right)^2 \left\{ \frac{\{1 - [v_f/(1 - v_f)]\rho^2\}^2}{[1 + \rho^2]^{3/2}} - 1 \right\} \right]. \quad (6)$$

Equation (6) will be the basis for our analysis, where, however, knowledge of the Young modulus E_f of the overlayer film is necessary.¹³ One can observe from Eq. (7) that for a flat film surface or equivalently $\rho=0$, Eq. (7) yields $\Delta\omega=0$ which is the correct asymptotic limit. In comparison the corresponding equation derived in Ref. 10 does not obey this constraint because during its derivation many terms, which were taken into account here, were omitted. In any case, for the calculation of the frequency shift $\Delta\omega/\omega$ from Eq. (6) the knowledge the local surface slope $\rho = \langle (\nabla h)^2 \rangle^{1/2}$ is necessary as it will be discussed in the following paragraph.

III. LOCAL SURFACE SLOPE AND SURFACE ROUGHNESS MODEL

The local surface slope $\rho = \langle (\nabla h)^2 \rangle^{1/2}$ in terms of Fourier-transform analysis is given by the expression¹⁴

$$\rho = \left(\int_0^{Q_c} q^2 \langle |h(q)|^2 \rangle d^2q \right)^{1/2} \quad (7)$$

with $\langle |h(q)|^2 \rangle$ the power roughness spectrum and $Q_c = \pi/a_o$ with a_o a minimum lateral roughness cutoff. Furthermore, a wide variety of deposited thin-film surfaces exhibit the so-called self-affine or power-law roughness.^{15–17} This type of roughness is characterized by the rms roughness amplitude w , the lateral correlation length ξ (indicating the average lateral feature size), and the roughness exponent $0 < H < 1$.^{15,16} Small values of H (~ 0) corresponds to jagged surfaces, while large values of H (~ 1) to a smooth hill valley morphology. An example is shown in Fig. 1(b) for a gold overlayer film with roughness ratio $w/\xi = 0.23$ and $H = 0.9$.

For self-affine roughness, the power spectrum obeys the scaling behavior $\langle |h(q)|^2 \rangle \propto q^{-2-2H}$ if $q\xi \gg 1$ and $\langle |h(q)|^2 \rangle \propto \text{const.}$ if $q\xi \ll 1$. This scaling is satisfied by the analytic model¹⁶

$$\langle |h(q)|^2 \rangle = \frac{aw^2\xi^2}{(1 + q^2\xi^2)^{1+H}}. \quad (8)$$

The parameter “ a ” in Eq. (8) is obtained by the normalization condition $\int_{0 < q < Q_c} q^2 \langle |h(q)|^2 \rangle d^2q = w^2$ yielding $a = (H/\pi) / [1 - (1 + Q_c^2\xi^2)^{-H}]$.¹⁶ This is equivalent to the fact that the height-height correlation $C(\vec{r}) = \langle (h(\vec{r})h(\vec{0})) \rangle = \int \langle |h(q)|^2 \rangle e^{-i\vec{q}\cdot\vec{r}} d^2q$ obeys the condition $C(\vec{r}=\vec{0}) = w^2$. Furthermore, substituting in Eq. (8) the roughness spectrum from Eq. (9) we obtain for the local slope the simple analytic expression

$$\rho = \frac{w}{\xi} \left\{ \frac{a\pi}{(1-H)} [(1 + Q_c^2\xi^2)^{1-H} - 1] - 1 \right\}^{1/2}. \quad (9)$$

The actual expressions in the limiting asymptotic cases $H=0$ and 1 can be obtained using the identity $\ln(x) = \lim_{c \rightarrow 0} (1/B)(x^B - 1)$. Therefore, we obtain in both cases for the local slope the more compact expressions: $\rho|_{H=1} = (w/\xi)[a \ln(1 + Q_c^2\xi^2) - 1]^{1/2}$ with $a|_{H=1} = (1/\pi)(1 + (Q_c\xi)^{-2})$, and $\rho|_{H=0} = (w/\xi)[a\pi(Q_c\xi)^2 - 1]^{1/2}$ with $a|_{H=0} = 1/[\pi \ln(1 + Q_c^2\xi^2)]$.

IV. RESULTS AND DISCUSSION

Our calculations were performed for relatively weak roughness or $\rho < 1$ corresponding to surface feature inclination angles $\theta = \tan^{-1}(\rho) < 45^\circ$. For the Lamé moduli we used the parameters, respectively, $\mu_s = -2.627$ GPa, and $\lambda_s = -2.70$ GPa, and for the Young modulus of the bare bulk cantilever (assuming that it is made from silicon) the value $E_s = 130$ GPa. For gold (Au) overlayer films we used the parameters $v_{fAu} = 0.44$, $E_{fAu} = 79$ GPa, and for Si overlayers the parameters $v_{Si} = 0.28$ and $E_{fSi} = 180$ GPa.

Calculations of the frequency shift ratio $\Delta\omega/\omega$ vs the local slope ρ are shown in Fig. 2 for two different cantilever thicknesses corresponding to different thickness ratios n ($=d/d_{ca}$). Indeed, as d_{ca} decreases it leads to significant increase of the roughness dependent frequency shift $\Delta\omega/\omega$ for relatively increased local surface slopes ($\rho > 0.5$). On the

other hand, if one increases the thickness d of the overlayer film, the influence on the ratio $\Delta\omega/\omega$ is far less significant as it is expected and illustrated in Fig. 3. Therefore, amplification of the roughness effect on $\Delta\omega/\omega$ can be more significant depending on the dimensions of the bare cantilever rather than the thickness of the overlayer film.

Moreover, as Fig. 2 shows the influence the bare cantilever thickness d_{ca} is more prominent for lower Poisson ratios ν_f and higher local surface slopes or equivalent rougher surfaces. As a matter of fact as Fig. 2 indicates a change in the Poisson ratio ν from that of gold ($\nu_f=0.44$) to that of silicon

($\nu_f=0.28$) for the overlayer film, and local slope values $\rho > 0.5$, the frequency shift $\Delta\omega/\omega$ can change more than a factor of five approaching that of an order of magnitude for surface slopes $\rho > 0.7$. On the other hand for very weak slopes, $\rho \ll 1$, if we consider the expansion $[1+\rho^2]^{3/2} \approx 1 + (3/2)\rho^2 \dots$ then we obtain from Eq. (6) up to second order a quadratic dependence on ρ ; $\Delta\omega/\omega \propto \rho^2$. In the more general case, by substituting Eq. (9) into Eq. (6), one obtains an analytic form for the frequency shift ratio $\Delta\omega/\omega$ as a function of the surface roughness parameters w , ξ , and H

$$\frac{\Delta\omega}{\omega} = \frac{2\mu_s + \lambda_s}{\tilde{E}_{sf,s}} \frac{6}{d_{ca}} \left(n + \frac{1}{2} \right)^2 \left\{ \frac{\left[1 - \frac{\nu_f}{1-\nu_f} \left(\frac{w}{\xi} \right)^2 \left\{ \frac{a\pi}{(1-H)} [(1+Q_c^2\xi^2)^{1-H} - 1] - 1 \right\} \right]^2}{\left[1 + \left(\frac{w}{\xi} \right)^2 \left\{ \frac{a\pi}{(1-H)} [(1+Q_c^2\xi^2)^{1-H} - 1] - 1 \right\} \right]^{3/2}} - 1 \right\}. \quad (10)$$

Equation (11) allows calculation of the roughness dependent frequency shift if one measures the surface roughness parameters w , ξ , and H by means, for example, correlation function measurement¹⁵⁻¹⁷ using atomic force microscopy scans [Fig. 1(b)].

In this respect, Fig. 4 shows the direct dependence of the frequency shift $\Delta\omega/\omega$ on the long wavelength roughness ratio w/ξ for various roughness exponents H . From Fig. 4 it is evident that if the corresponding curve has a maximum, then we can only consider as a valid regime the one prior to the maximum in order to avoid to crossover into the regime with large local slopes ($\rho > 1$). To clarify this point we show in the inset of Fig. 4 the dependence of the local slope ρ vs the roughness ratio w/ξ for the two distinct roughness exponents H used for the calculations of $\Delta\omega/\omega$. For both cases of different cantilever thicknesses the requirement $\rho < 1$ translates, respectively, to roughness ratios $w/\xi < 0.1$ if $H=0.6$, and $w/\xi < 0.3$ if $H=0.9$. Clearly if the exponent H becomes smaller or equivalently the surface becomes rougher at short length scales ($< \xi$), the influence on the frequency shift can increase drastically for thinner made cantilevers.

The previous illustrative calculations of the roughness effect on $\Delta\omega/\omega$ indicate that changes in the cantilever frequency due to surface roughness is a factor that requires attention especially for high frequency cantilevers in the megahertz (MHz) range and above. If we consider for example in Fig. 4 the roughness ratio $w/\xi=0.23$ and $H=0.9$ [Fig. 1(b)], which are parameters typically observed for gold overlayers [Fig. 1(b)], the frequency shift for 1- μm -thick cantilever with vibration frequency $\omega=1$ MHz is $\Delta\omega \sim 100$ Hz while for an 4- μm -thick cantilever the frequency shift is $\Delta\omega \sim 10-20$ Hz. These values can be significant in high precision sensing applications such as force sensing in ultrahigh vacuum conditions, where changes in the frequency are directly related to the gradient of acting forces

($\Delta\omega \propto \nabla F$) in terms of frequency-modulation schemes.^{18,19}

V. CONCLUSIONS

In summary we investigated the influence of random roughness on the vibration frequency of cantilevers coated with thin film overlayers. Initially we derived the necessary expressions for the surface roughness-induced frequency shift $\Delta\omega/\omega$. Subsequently it was illustrated that this shift depends on the particular roughness parameters (assuming the general case of self-affine rough surfaces), the material properties of the deposited overlayer film, and the dimensions mainly of the bare cantilever (which linearly amplify the roughness effect). Indeed, it was shown that the roughness influence becomes significant for thin cantilevers ($\leq 1 \mu\text{m}$), and significant local surface slopes (> 0.5) within the limits of applicability of the proposed formalism. Finally, as it was discussed, our results can be of importance for high-precision frequency sensing applications (using high-frequency cantilevers) in the field of micro/nanomechanics.

ACKNOWLEDGMENTS

The authors would like to acknowledge financial support by the STW under Grant No. 10082. We would like to thank J. Weissmuller who brought us to our attention the article Mechanics of corrugated surfaces in Ref. 5(b).

APPENDIX

1. Equation of cantilever motion

The general equation of cantilever motion derived in Ref. 10 has the form

$$\begin{aligned}
 & \frac{\partial^2}{\partial x^2} \left(\left\{ \frac{\tilde{E}_s d_{ca}^3}{12} + \frac{\tilde{E}_f d_{ca}^3}{3} \left[\left(n + \frac{1}{2} \right)^3 - \frac{1}{8} \right] \right. \right. \\
 & \quad \left. \left. + (2\mu_s + \lambda_s) d_{ca}^2 \left(n + \frac{1}{2} \right)^2 \frac{[1 - (v_f/1 - v_f)(\nabla h)^2]^2}{[1 + (\nabla h)^2]^{3/2}} \right\} \frac{\partial^2 Z}{\partial x^2} \right) \\
 & \quad + d_{ca} \left[(\rho_s + \rho_f n) \frac{\partial^2 Z}{\partial t^2} \right] \\
 & = \tau_o d_{ca} \frac{\partial^2}{\partial x^2} \left\{ \frac{\left(n + \frac{1}{2} \right) [1 - (v_f/1 - v_f)(\nabla h)^2]}{[1 + (\nabla h)^2]^{3/2}} \right\} \quad (A1)
 \end{aligned}$$

If we consider a slow roughness variation then substitution of the term $(\nabla h)^2$ in Eq. (A1) with its average value $\langle (\nabla h)^2 \rangle$ (Ref. 10) yields Eq. (1). Under these conditions the term on the right hand side of Eq. (A1) gives only zero contribution.¹⁰

2. Calculation of total frequency shift

In order to calculate the frequency shift due to the overlayer film on top of the cantilever we consider the equation

of motion for flat surfaces, Eq. (4), and that of a bare cantilever

$$\frac{\tilde{E}_s d_{ca}^3}{12} \frac{\partial^4 Z}{\partial x^4} + \tilde{\mu}^o \frac{\partial^2 Z}{\partial t^2} = 0 \quad (A2)$$

with $\tilde{\mu}^o = d_{ca} \rho_s$. Since the vibration frequencies of the bare cantilever and film/cantilever are given by $\omega_o^2 = C\tilde{E}_s(d_{ca}^3/12)/\tilde{\mu}^o$ and $\omega^2 = C\tilde{E}_{sf,s}(d_{ca}^3/12)/\tilde{\mu}$ respectively, if we consider the expansion $\omega^2 \approx \omega_o^2 + 2\omega_o \Delta\omega_o$ (assuming $\Delta\omega_o \ll \omega$) we obtain the frequency shift $\Delta\omega_o/\omega_o$ due to the deposited film

$$\frac{\Delta\omega_o}{\omega_o} = \frac{1}{2} \left(\frac{\tilde{\mu}^o \tilde{E}_{sf,r}}{\tilde{\mu} \tilde{E}_s} - 1 \right). \quad (A3)$$

Finally, if we consider Eqs. (6) and (A3), the total frequency shift $\Delta\omega_{tot}/\omega_o$ due to the overlayer film and surface roughness is given by

$$\frac{\Delta\omega_{tot}}{\omega_o} = \left(\frac{\Delta\omega_o}{\omega_o} \right) + \left(\frac{\omega}{\omega_o} \right) \left(\frac{\Delta\omega}{\omega} \right). \quad (A4)$$

Finally, substitution from Eqs. (A3) and (10) yields also the analytic form

$$\frac{\Delta\omega_{tot}}{\omega_o} = \frac{1}{2} \left(\frac{\rho_s}{\rho_s + n\rho_f} \frac{\tilde{E}_{sf,r}}{\tilde{E}_s} - 1 \right) + \left(\frac{\omega}{\omega_o} \right) \frac{2\mu_s + \lambda_s}{\tilde{E}_{sf,s}} \frac{6}{d_{ca}} \left(n + \frac{1}{2} \right)^2 \left\{ \frac{\left[1 - \frac{v_f}{1 - v_f} \left(\frac{w}{\xi} \right)^2 \left\{ \frac{a\pi}{(1-H)} [(1 + Q_c^2 \xi^2)^{1-H} - 1] - 1 \right\} \right]^2}{\left[1 + \left(\frac{w}{\xi} \right)^2 \left\{ \frac{a\pi}{(1-H)} [(1 + Q_c^2 \xi^2)^{1-H} - 1] - 1 \right\} \right]^{3/2}} - 1 \right\}. \quad (A5)$$

*Corresponding author; g.palasantzas@rug.nl

¹A. B. Hutchinson, P. Truitt, L. Sekaric, J. M. Parpia, H. G. Craighead, J. E. Butler, and K. C. Schwab, *Appl. Phys. Lett.* **84**, 972 (2004); A. N. Cleland and M. L. Roukes, *ibid.* **69**, 2653 (1996); K. L. Ekinci and M. L. Roukes, *Rev. Sci. Instrum.* **76**, 061101 (2005); K. L. Ekinci, Y. T. Yang, X. M. H. Huang, and M. L. Roukes, *Appl. Phys. Lett.* **81**, 2253 (2002); K. L. Ekinci, Y. T. Yang, and M. L. Roukes, *J. Appl. Phys.* **95**, 2682 (2004); K. C. Schwab and M. L. Roukes, *Phys. Today* **58**(7), 36 (2005).

²V. Sazonova, Y. Yaish, H. Ustunel, D. Roundy, T. A. Arias, and P. L. McEuen, *Nature (London)* **431**, 284 (2004); K. Y. Yasumura, T. D. Stowe, E. M. Chow, T. Pfafman, T. W. Kenny, B. C. Stipe, and D. Rugar, *J. Microelectromech. Syst.* **9**, 117 (2000); D. W. Carr, S. Evoy, L. Sekaric, H. G. Craighead, and J. M. Parpia, *Appl. Phys. Lett.* **75**, 920 (1999); S. Evoy, A. Olkhovets, L. Sekaric, J. M. Parpia, and H. G. Craighead, *ibid.* **77**, 2397 (2000).

³N. V. Lavrik, M. J. Sepaniak, and P. G. Datskos, *Rev. Sci. Instrum.* **75**, 2229 (2004); G. Y. Chen, T. Thundat, E. A. Wachter,

and R. J. Warmack, *J. Appl. Phys.* **77**, 3618 (1995); G. Wu, H. Ji, K. Hansen, T. Thundat, R. Datar, R. Cote, M. F. Hagan, A. K. Chakraborty, and A. Majumdar, *Proc. Natl. Acad. Sci. U.S.A.* **98**, 1560 (2001); S. Cherian and T. Thundata, *Appl. Phys. Lett.* **80**, 2219 (2002).

⁴M. E. Gurtin, X. Markenscoff, and R. N. Thurston, *Appl. Phys. Lett.* **29**, 529 (1976).

⁵J. Weissmüller and H. L. Duan, *Phys. Rev. Lett.* **101**, 146102 (2008); for a general overview on the mechanics of corrugated surfaces see also: Y. Wang, J. Weissmüller, and H. L. Duan, *J. Mech. Phys. Sol.* (to be published); J. Weissmüller (private communication).

⁶Y. Wang, J. Weissmüller, and H. L. Duan, *Appl. Phys. Lett.* **96**, 226101 (2010); O. Ergincan, G. Palasantzas, and B. J. Kooi, *Appl. Phys. Lett.* **96**, 226102 (2010).

⁷N. V. Lavrik, C. A. Tipple, M. J. Sepaniak, and P. G. Datskos, *Chem. Phys. Lett.* **336**, 371 (2001); *Biomed. Microdevices* **3**, 35 (2001).

⁸A. Fabre, E. Finot, J. Demoment, and S. Contreras, *Ultramicros-*

- copy **97**, 425 (2003).
- ⁹R. Desikan, I. Lee, and T. Thundat, *Ultramicroscopy* **106**, 795 (2006); M. Godin, P. J. Williams, V. Tabard-Cossa, O. Laroche, L. Y. Beaulieu, R. B. Lennox, and P. Grutter, *Langmuir* **20**, 7090 (2004).
- ¹⁰H. L. Duan, Y. Xue, and X. Yi, *Acta Mech. Solida Sinica* **22**, 550 (2009).
- ¹¹H. L. Duan, J. Wang, Z. P. Huang, and B. L. Karihaloo, *J. Mech. Phys. Solids* **53**, 1574 (2005).
- ¹²J. E. Sader, *J. Appl. Phys.* **84**, 64 (1998).
- ¹³J. D. Shi, K.-H. Wu, and G. Larkins, *Mater. Charact.* **38**, 301 (1997).
- ¹⁴G. Palasantzas, *Phys. Rev. E* **56**, 1254 (1997).
- ¹⁵J. Krim and G. Palasantzas, *Int. J. Mod. Phys. B* **9**, 599 (1995); P. Meakin, *Phys. Rep.* **235**, 189 (1993); Y.-P. Zhao, G.-C. Wang, and T.-M. Lu, *Characterization of Amorphous and Crystalline Rough Surfaces-Principles and Applications*, Experimental Methods in the Physical Science Vol. 37 (Academic Press, New York, 2001).
- ¹⁶G. Palasantzas, *Phys. Rev. B* **48**, 14472 (1993); **49**, 5785 (1994).
- ¹⁷G. Palasantzas and J. Krim, *Phys. Rev. Lett.* **73**, 3564 (1994).
- ¹⁸G. Torricelli, P. J. van Zwol, O. Shpak, C. Binns, G. Palasantzas, B. J. Kooi, V. B. Svetovoy, and M. Wuttig, *Phys. Rev. A* **82**, 010101(R) (2010); G. Torricelli, S. Thornton, C. Binns, I. Pirozhenko, and A. Lambrecht, *J. Vac. Sci. Technol. B* **28**, C4A30 (2010).
- ¹⁹F. J. Giessibl, *Rev. Mod. Phys.* **75**, 949 (2003); R. García and R. Pérez, *Surf. Sci. Rep.* **47**, 197 (2002).